

- (8) Cheng, P.-L. Sc.D. Thesis, Massachusetts Institute of Technology, 1988.
- (9) Morton, M.; Fetters, L. *Rubber Chem. Technol.* **1975**, *48*, 359.
- (10) Gilman, H.; Cartledge, F. K. *J. Organomet. Chem.* **1964**, *2*, 447.
- (11) Glinka, C. J. *AIP Conf. Proc.* **1981**, *89*, 395.
- (12) Amis, E. J.; Glinka, C. J.; Han, C.; Hasagawa, H.; Hashimoto, T.; Lodge, T.P.; Matsushita, Y. *Polym. Prepr. (Am. Chem. Soc., Div. Polym. Chem.)* **1983**, *24*, 215.
- (13) Jahshan, S. N.; Summerfield, G. C. *J. Polymer. Sci., Polym. Phys. Ed.* **1980**, *18*, 1859.
- (14) Kinning, D. J.; Thomas, E. L. *Macromolecules* **1984**, *17*, 1712.
- (15) Percus, J. K.; Yevick, G. J. *Phys. Rev.* **1958**, *110*, 1.

## A New Look at the "Run Number" Concept in Copolymer Characterization

**J. C. Randall\* and C. J. Ruff**

*Baytown Polymers Center, Exxon Chemical Company, Baytown, Texas 77522.*

*Received March 1, 1988*

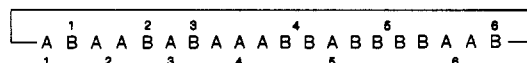
**ABSTRACT:** The "run number", introduced by Harwood and Ritchey in 1964, is reviewed in this study in light of developments in instrumentation, which now permit run number measurements. The concept is extended to include measurements of "chain punctuation" in semicrystalline polymers, that is, the number of sequences per 100 repeat units that have the capability for crystallization. Intervening sequences, incapable of crystallization, are regarded as chain punctuating units. The "sequence number" is also introduced as an adjunct to the "run number". It is simply the total number of sequences per 100 repeat units of a particular type and includes sequence lengths of one to whatever is the longest sequence length in the copolymer chain.

### Introduction

The concept of "run number", which describes the number of times per 100 repeat units a copolymer chain switches from one type of comonomer unit to the other, was introduced by Harwood and Ritchey in 1964.<sup>1</sup> The run number approach to copolymer characterization was developed at a time when it could not be tested because the required experimental data were not available. It was only in the early 1970s with the advent of carbon-13 NMR spectroscopy that *n*-ad distributions in copolymers could be measured and the "run number" concept evaluated. By that time the run number concept was buried deeply in the polymer literature and was essentially waiting to be rediscovered. The first to reexamine the run number was Randall and Hsieh,<sup>2</sup> who demonstrated that observed densities versus run numbers for a series of linear low density polyethylenes gave a single uniform relationship in the 0.920–0.940 density range inspite of differences in branch lengths. The use of "run number" takes into account branches on adjacent repeat units, which allows the number of times the chains are "punctuated" by contiguous units to be determined. The mole percent of comonomer incorporated may or may not reflect the true chain punctuation. It will depend upon the precise manner in which the comonomer repeat units are incorporated. The observed densities in this earlier study were found to be more closely related to the run number than to the overall comonomer contents, which gave a less definitive relationship. The "run number" versus density correlation was also independent of branch length for ethyl, butyl, and hexyl branches.<sup>2</sup> In polymerizations utilizing the classical titanium based Ziegler catalyst system, it is often noted that 1-octene is more efficient than 1-hexene, which, in turn, is more efficient than 1-butene in depressing the density of ethylene-1-olefin copolymers. This hierarchy of efficiency may be related more to a tendency to form both contiguous and alternating 1-olefin derived repeat units, a property resulting from the catalyst used, than to the length of the branch. There may be a small contribution from branch length but it appears to be less sig-

nificant than the effects from "clustering" and alternation of 1-olefin derived repeat units. Because of the possible new insights gained through the use of the "run number" in copolymer characterization, the run number concept and chain punctuation were explored further in this study.

Harwood and Ritchey defined the "run number" as the percent (AB + BA) diads, which gives the number of A to B plus B to A alternations per 100 copolymer chain units.



In the above sequence,<sup>1</sup> there are 6 "A" runs and 6 "B" runs giving 12 (AB + BA) diads within a sequence of 20 units, which lead to a Harwood and Ritchey "run number" of 60. Note that the ends of the above chain are connected to approximate a long chain, thus precluding the necessity for taking end unit differences into consideration.

In this study, we wish to demonstrate the utility of the "sequence number" when defining chain punctuation. In their original description of "run number", Harwood and Ritchey expressed the total number of times per 100 units an alternation occurred from either A to B or B to A. It may be more meaningful to identify the number of times per 100 repeat units runs of length one or more of a particular type of repeat unit *punctuate* a chain of repeat units of the other type. Note in the above example that the total series of A repeat units is punctuated six times by "B" sequences, and likewise the series of B repeat units is punctuated six times by "A" sequences. The number of "A" sequences must necessarily equal the number of "B" sequences for any copolymer chain that starts with an "A" and ends with a "B" and vice versa. For copolymer chains with like end units, either A or B, the number of "A" sequences will be within plus or minus one of the number of "B" sequences. For high degrees of alternations, the numbers of "A" and "B" sequences, therefore, become essentially the same regardless of whether the end units are alike or different. It is this view of chain punctuation that may be more useful than the "run number", which is

simply the sum of the "A" and "B" sequence numbers. In the previous example, the "A" sequence number equals the "B" sequence number, which is 30. Experimentally, the "A" sequence number can often be determined independently of the "B" sequence number, thus giving an independent check of the sequence number. In their discussion of the "run number", Harwood and Ritchey also defined the run number in terms of reactivity ratios and probability statistics and believed the concept to offer a useful and convenient parameter for characterizing copolymer sequence distributions.<sup>1</sup>

There are several advantages in using the "sequence number" in place of Harwood and Ritchey's "run number". When there are no contiguous pairs of "B" repeat units in a copolymer consisting predominantly of "A" units, the "sequence number" will be the same as the mole percent "B" in the copolymer. Any deviation of the "sequence number" from the mole percent "B" will indicate that "clustering" of the "B" units has occurred.

The "sequence number", as well as the "run number", is also useful for identifying the type of copolymer. A 50:50 A/B copolymer, for example, will give a sequence number of 0.5 for the diblock copolymer, a value of 25 will be obtained for a statistically random copolymer and the perfectly alternating copolymer will give a sequence number of 50. Finally, the average "A" and "B" sequence lengths are determined after dividing the mole percent "A" and mole percent "B", respectively, by the sequence number.

The "A" and "B" sequence numbers can be expressed as series, as follows

"B" sequence number =

$$[ABA + ABBA + ABBBA + \dots + A(B)_nA] \quad (1)$$

$$\text{"B" sequence number} = [ABA + \frac{1}{2}(ABB + BBA)] =$$

$$\frac{1}{2}[AB + BA] \quad (2)$$

and conversely

"A" sequence number =

$$[BAB + BAAB + BAAAB + \dots + B(A)_nB] \quad (3)$$

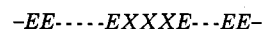
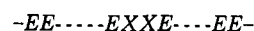
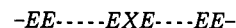
$$\text{"A" sequence number} = [BAB + \frac{1}{2}(BAA + AAB)] =$$

$$\frac{1}{2}[AB + BA] \quad (4)$$

Note that in the above equations, the "A" and "B" sequence numbers are defined per chain and the equations are written in a form usual for the "necessary relationships",<sup>3,4</sup> that is, "ABA" etc. represents both the sequence length and its concentration. It is apparent from eq 2 and 4 that a measurement of a complete triad distribution leads to independent determinations of the "A" and "B" sequence numbers. For most copolymers, a diad or triad distribution can readily be measured by carbon-13 NMR. In general, the sequence number concept is worthy of further evaluation because it offers a measure of chain punctuation, which, in turn, can be related to polymer crystallinity and any property that is a direct function of crystallinity.

In this study, a series of ethylene-1-olefin copolymers, derived from 1-butene, 1-hexene, and 1-octene comonomers, have been characterized by density measurements and by carbon-13 NMR. With only a few exceptions, the 1-olefin concentrations remain below 10 mol % and it is of interest to establish how the sequence numbers relate to the observed densities. The copolymer density should be represented by some function of the number of times the ethylene sequences are punctuated by either solitary, contiguous, or other ethylene chain disrupting sequences of 1-olefin units and not necessarily by the overall mole

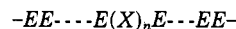
percent 1-olefin.<sup>2</sup> The solitary and contiguous 1-olefin (X) units, acting as single chain punctuating sequences, are



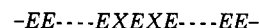
.

.

.



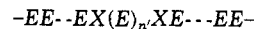
In addition to contiguous 1-olefin sequences, there are other combinations of ethylene and 1-olefin repeat units that also serve as single-chain punctuating sequences and must be considered when one is comparing chain punctuation to polymer crystallinity. These are



.

.

.



where "n" is defined as the maximum number of contained ethylene units between branches that will not crystallize under any conditions. The concentrations of the first two terms in the above series, XEX and XEEEX, can be conveniently measured from carbon-13 NMR spectra.<sup>5-7</sup> Unfortunately, a sequence of three ethylene repeat units between 1-olefin units cannot be distinguished from those that are longer utilizing carbon-13 NMR. Although XEX and XEEEX are the most significant of the  $X(E)_nX$  contributors to chain punctuation, they still comprise less than 10% of the observed sequence number. To define chain punctuation completely, one must obtain the collective concentrations of  $X(E)_nX$  sequences from  $n = 1$  to  $n = n'$ . There is no available method that permits the concentrations of all of these latter chain punctuating sequences to be measured. The usual approach is to determine these concentrations statistically once an appropriate statistical model has proven applicable. Finally, samples that did not vary substantially in molecular weight were selected for comparing chain punctuation with some experimental measure of crystallinity. This approach was taken to avoid any possible contributions to the observed crystallinity that may have been created by molecular weight differences.

## Experimental Section

Carbon-13 NMR spectra were obtained on a Varian XL-200 NMR spectrometer. Acquisition conditions were as follows: pulse angle, 90°; pulse delay, 10 s; acquisition time, 1 s; sweep width, 8000 Hz; the nominal number of FID's collected per sample, 5000. Broad-band proton noise decoupling was utilized during data acquisition and perdeuteriobenzene was used as an internal lock signal. Each sample was dissolved at 15 wt % in 1,2,4-trichlorobenzene, and the probe temperature was maintained at  $125 \pm 0.2$  °C.

The determination of the triad distributions for the various 1-olefin copolymers in principle followed the methods reported previously<sup>6,7</sup> with the exception that the E-centered triads were determined experimentally independently from the X-centered triads as opposed to invoking the appropriate necessary relationships and utilizing fewer experimental observations. This approach permitted the sequence numbers to be determined independently, thus verifying the experimental method. The X- and E-centered sequence numbers differed only by an average of 2.4% with the differences ranging from 0 to 5.6%. Gated decoupling experiments also demonstrated that the analytical results were not influenced by differences among nuclear Overhauser effects. The experimentally determined triad distributions

Table I  
Observed and Calculated Triad Distributions Based on Corresponding Bernoullian and First-Order Markovian Models for  
Ethylene-1-Butene, Ethylene-1-Hexene, and Ethylene-1-Octene Copolymers

	comonomer	EEE	XEE + EEX	XEX	XEX	EXX + XXE	XXX	$2X(EE)/E(EX + XE)$
A	1-butene	0.898	0.066	0.001	0.033	0.002	0.000	0.97
	bern	0.901	0.064	0.001	0.032	0.002	0.000	1.00
	1st ord	0.897	0.067	0.001	0.034	0.002	0.000	0.99
B	1-butene	0.830	0.108	0.005	0.050	0.007	0.001	0.95
	bern	0.839	0.101	0.003	0.050	0.006	0.000	1.00
	1st ord	0.823	0.110	0.004	0.055	0.008	0.000	1.01
C	1-butene	0.869	0.084	0.003	0.040	0.003	0.002	0.98
	bern	0.872	0.081	0.002	0.041	0.004	0.000	1.00
	1st ord	0.864	0.086	0.002	0.042	0.006	0.000	1.02
D	1-butene	0.841	0.100	0.004	0.053	0.001	0.000	0.95
	bern	0.844	0.098	0.003	0.049	0.006	0.000	1.00
	1st ord	0.840	0.102	0.003	0.054	0.001	0.000	0.96
E	1-butene	0.856	0.090	0.002	0.047	0.005	0.000	1.03
	bern	0.851	0.094	0.003	0.047	0.005	0.000	1.00
	1st ord	0.858	0.090	0.002	0.045	0.005	0.000	1.00
F	1-butene	0.813	0.113	0.006	0.063	0.005	0.000	0.99
	bern	0.810	0.118	0.004	0.059	0.009	0.000	1.00
	1st ord	0.814	0.117	0.004	0.061	0.004	0.000	0.97
G	1-butene	0.795	0.129	0.006	0.064	0.005	0.000	0.94
	bern	0.806	0.120	0.005	0.060	0.009	0.000	1.00
	1st ord	0.792	0.130	0.005	0.068	0.005	0.000	0.96
H	1-butene	0.505	0.270	0.043	0.161	0.021	0.000	0.81
	bern	0.548	0.244	0.027	0.122	0.054	0.006	1.00
	1st ord	0.497	0.277	0.039	0.167	0.021	0.001	0.83
I	1-hexene	0.998	0.001	0.000	0.001	0.000	0.000	1.00
	bern	0.998	0.001	0.000	0.001	0.000	0.000	1.00
	1st ord	0.998	0.001	0.000	0.001	0.000	0.000	1.00
J	1-hexene	0.928	0.045	0.002	0.023	0.002	0.000	1.00
	bern	0.927	0.047	0.001	0.024	0.001	0.000	1.00
	1st ord	0.925	0.048	0.001	0.023	0.003	0.000	1.04
K	1-hexene	0.914	0.053	0.002	0.028	0.003	0.000	1.03
	bern	0.910	0.058	0.001	0.029	0.002	0.000	1.00
	1st ord	0.913	0.056	0.001	0.028	0.003	0.000	1.02
L	1-hexene	0.889	0.071	0.003	0.034	0.003	0.000	0.96
	bern	0.893	0.069	0.001	0.034	0.003	0.000	1.00
	1st ord	0.885	0.074	0.002	0.037	0.003	0.000	1.00
M	1-hexene	0.908	0.058	0.002	0.030	0.003	0.000	1.00
	bern	0.906	0.060	0.001	0.030	0.002	0.000	1.00
	1st ord	0.906	0.060	0.001	0.030	0.003	0.000	1.01
N	1-hexene	0.886	0.070	0.004	0.036	0.005	0.000	0.99
	bern	0.885	0.073	0.002	0.037	0.003	0.000	1.00
	1st ord	0.882	0.075	0.002	0.038	0.004	0.000	1.00
O	1-hexene	0.886	0.071	0.005	0.035	0.004	0.000	0.97
	bern	0.887	0.072	0.001	0.036	0.003	0.000	1.00
	1st ord	0.880	0.077	0.002	0.038	0.004	0.000	1.01
P	1-hexene	0.888	0.067	0.005	0.036	0.004	0.000	1.01
	bern	0.884	0.074	0.002	0.037	0.003	0.000	1.00
	1st ord	0.885	0.074	0.002	0.036	0.004	0.000	1.01
Q	1-hexene	0.869	0.080	0.006	0.040	0.004	0.000	0.95
	bern	0.873	0.081	0.002	0.040	0.004	0.000	1.00
	1st ord	0.862	0.088	0.002	0.044	0.004	0.000	1.00
R	1-hexene	0.880	0.074	0.004	0.038	0.003	0.000	0.98
	bern	0.881	0.076	0.002	0.038	0.003	0.000	1.00
	1st ord	0.877	0.079	0.002	0.039	0.004	0.000	1.00
S	1-hexene	0.889	0.067	0.002	0.037	0.004	0.000	1.07
	bern	0.880	0.077	0.002	0.038	0.003	0.000	1.00
	1st ord	0.891	0.069	0.001	0.034	0.004	0.000	1.02
T	1-hexene	0.904	0.059	0.002	0.034	0.002	0.000	1.05
	bern	0.897	0.066	0.001	0.033	0.003	0.000	1.00
	1st ord	0.906	0.061	0.001	0.031	0.002	0.000	0.99
V	1-hexene	0.805	0.120	0.006	0.062	0.007	0.000	1.04
	bern	0.808	0.119	0.004	0.060	0.009	0.000	1.00
	1st ord	0.802	0.123	0.005	0.063	0.007	0.000	0.98
U	1-octene	0.883	0.073	0.002	0.037	0.003	0.001	1.02
	bern	0.881	0.076	0.002	0.038	0.003	0.000	1.00
	1st ord	0.882	0.075	0.002	0.037	0.005	0.000	1.02
W	1-octene	0.953	0.030	0.000	0.017	0.000	0.000	1.03
	bern	0.951	0.032	0.000	0.016	0.001	0.000	1.00
	1st ord	0.955	0.030	0.000	0.015	0.000	0.000	0.99
X	1-octene	0.923	0.048	0.002	0.028	0.000	0.000	1.02
	bern	0.918	0.053	0.001	0.026	0.002	0.000	1.00
	1st ord	0.924	0.050	0.001	0.025	0.000	0.000	0.98

Table I (Continued)

	EEE	XEE + EEX	XEX	EXE	EXX + XXE	XXX	2X(E E)/E(EX + XE)
comonomer <sup>a</sup>	000	001 + 100	101	010	011 + 110	111	2(1)(00)/(1)(10 + 01)
HPB-1.262	0.760	0.156	0.000	0.078	0.006	0.000	0.97
bern	0.769	0.141	0.006	0.070	0.013	0.001	1.00
1st ord	0.768	0.143	0.007	0.074	0.008	0.000	0.97
HPB-1.015	0.532	0.284	0.020	0.142	0.022	0.000	0.84
bern	0.584	0.229	0.022	0.115	0.045	0.004	1.00
1st ord	0.541	0.260	0.031	0.155	0.013	0.000	0.84
HPB-1.387	0.432	0.244	0.084	0.158	0.042	0.030	0.85
bern	0.456	0.273	0.041	0.136	0.081	0.012	1.00
1st ord	0.420	0.286	0.049	0.149	0.085	0.005	0.96
HPB-1.086	0.330	0.295	0.064	0.170	0.074	0.064	0.58
bern	0.331	0.295	0.066	0.147	0.131	0.029	1.00
1st ord	0.328	0.294	0.066	0.144	0.136	0.032	1.04
HPB-1.291	0.128	0.272	0.127	0.180	0.238	0.055	0.84
bern	0.146	0.262	0.118	0.131	0.236	0.106	1.00
1st ord	0.136	0.272	0.135	0.161	0.220	0.075	0.84

<sup>a</sup> Abbreviations: 0, hydrogenated 1,4-butadiene repeat unit; 1, hydrogenated 1,2-butadiene repeat unit.

Table II  
Structure/Property Data for Ethylene-1-Butene,  
Ethylene-1-Hexene, and Ethylene-1-Octene Copolymers

comonomer	d, g cm <sup>-3</sup>	mol % 1-olefin	sequence no.		%	cryst	η <sub>E</sub>
			"E"	"X"			
A	1-butene	0.920	3.4	3.4	3.3	42	29
B	1-butene	0.918	5.7	5.9	5.3	41	17
C	1-butene	0.918	4.4	4.5	4.1	41	22
D	1-butene	0.913	5.5	5.4	5.4	37	18
E	1-butene	0.911	5.2	4.7	5.0	36	20
F	1-butene	0.908	6.8	6.2	6.6	34	15
G	1-butene	0.904	7.0	7.1	6.7	31	13
H	1-butene	0.887	18.2	17.8	17.1	19	5
I	1-hexene	0.955	0.1	0.1	0.1	66	
J	1-hexene	0.930	2.5	2.5	2.4	49	40
K	1-hexene	0.922	3.1	2.9	3.0	43	33
L	1-hexene	0.920	3.7	3.8	3.6	42	26
M	1-hexene	0.920	3.2	3.1	3.1	42	31
N	1-hexene	0.919	4.0	3.9	3.8	41	25
O	1-hexene	0.919	3.9	4.0	3.7	41	25
P	1-hexene	0.919	4.0	3.8	3.8	41	25
Q	1-hexene	0.918	4.4	4.6	4.2	41	22
R	1-hexene	0.918	4.1	4.1	4.0	41	24
S	1-hexene	0.918	4.2	3.6	4.0	41	25
T	1-hexene	0.918	3.6	3.1	3.5	40	29
V	1-hexene	0.899	6.9	6.6	6.5	27	14
Z	1-octene	0.930	1.3	1.5	1.3	49	76
W	1-octene	0.926	1.9	2.1	1.9	46	52
Y	1-octene	0.926	1.8	1.5	1.7	46	58
X	1-octene	0.918	2.8	2.6	2.8	41	36
U	1-octene	0.916	4.1	3.9	3.9	39	25

Graessley Data, Hydrogenated Polybutadienes<sup>9</sup>

HPB-1.262	0.910 <sub>5</sub>	8.4	7.8	8.1	35	11.3
HPB-1.015	0.895	16.4	16.2	15.3	24	5.5
HPB-1.387	0.884 <sub>5</sub>	23.0	17.9	18.4	17	4.2
HPB-1.086	0.877	30.8	20.7	20.9	12	3.3
HPB-1.291	0.862 <sub>5</sub>	47.3	26.3	29.9	2	1.8

as well as statistical fits for each of the copolymer systems are given in Table I.

Characterization data, including mole percent of 1-olefin, sequence numbers, average ethylene sequence length, density, and percent crystallinity as determined from the densities, are given in Table II for a series of ethylene-1-butene, ethylene-1-hexene, and ethylene-1-octene copolymers. The average ethylene sequence lengths were obtained by dividing the various mole percents of ethylene by the corresponding sequence numbers in column 4. Data for a series of hydrogenated polybutadienes were available from the literature<sup>9</sup> and are included for comparison. Graessley<sup>9</sup> kindly provided the original triad distributions obtained from carbon-13 NMR spectra. The sequence distributions of the hydrogenated polybutadienes were found to be statistically random. The ethylene-1-olefin copolymers are expected to give sequence distributions that vary broadly in scope because both commercial

and experimental copolymers, prepared with a wide variety of catalyst systems, are represented.

Density measurements were made on compression molded samples by using a density gradient column following ASTM procedure D1505, which ensures uniform thermal histories for all of the samples. Briefly, each sample was preheated at 215 °C for 5 min and then subjected to the low-pressure cycle of the compression molding procedure for 1 min and the high-pressure cycle for 5 min. Each sample was then cooled to 29 °C at a rate of 8.3 deg/min. After removal from the press, the samples were allowed to age for 40 h before density measurements were made.

Either molecular weight or melt index data were available for all of the samples. The majority of the samples had weight average molecular weights between 75 000 and 115 000 with  $M_w/M_n$  ratios ranging from 2.0 to 3.5.

## Results and Discussion

For a given set of crystallization conditions, one expects to find some minimum ethylene sequence length between branches where crystallization first occurs in an ethylene-1-olefin copolymer. The longest ethylene sequence length that fails to crystallize under any condition has been previously defined as  $n'$ . It is expressed in the following equations for the sequence number and total ethylene content: sequence number = number of crystallizable sequences plus number of uncrystallizable sequences

$$\text{sequence number} = \sum_{n_1=1}^{n_1=n'} [X(E)_{n_1}X] + \sum_{n_2=n'+1}^{n_2=m} [X(E)_{n_2}X] \quad (5)$$

$$\text{sequence number} = \frac{1}{2}[XE + EX]$$

$$\text{sequence number} = [XEX] + \frac{1}{2}[XEE + EEX] = [EXE] + \frac{1}{2}[EXX + XXE]$$

total E content = content of E in crystallizable sequences + content of E in noncrystallizable sequences

$$\text{total E content} = \sum_{n_1=1}^{n_1=n'} n_1[X(E)_{n_1}X] + \sum_{n_2=n'+1}^{n_2=m} n_2[X(E)_{n_2}X] \quad (6)$$

$$\text{total E content} = (EE) + \frac{1}{2}(XE + EX)$$

$$\text{total E content} = (EEE) + (XEE + EEX) + (XEX)$$

where, in both eq 5 and 6, the sum over  $n_1$  occurs from 1 to  $n'$  and the sum over  $n_2$  occurs from  $n' + 1$  to " $m$ ", the longest uninterrupted ethylene sequence in the copolymer chain. Equation 5 can be used to determine either the fraction or the number of sequences capable of crystallization per 100 chain units, and equation 6 can be used to determine the fraction of ethylene in sequences capable

of crystallization. This fraction of "crystallizable ethylene" will be examined initially. After dividing eq 6 through by the total  $E$  content, we have defined the fraction of ethylene in sequences capable of crystallization versus that in sequences which will not crystallize under any conditions. The fraction of sequences capable of crystallization is expected to exhibit some relationship to the observed density. One way this relationship can be defined is to use the observed density to determine the percent crystallinity<sup>8</sup>

$$100 \left[ \frac{d_{\text{obsd}} - d_0}{d_{100} - d_0} \right] = \% \text{ crystallinity} \quad (7)$$

where  $d_{100}$  is the density when 100% of the ethylene sequences crystallize and  $d_0$  is the density of a totally amorphous ethylene-1-olefin copolymer where none of the ethylene sequences are capable of crystallization. Values for  $d_{100}$  have been reported in the literature and 1.003 was used in this study.<sup>8</sup> An appropriate ethylene-1-olefin rubber or amorphous copolymer can be used to determine  $d_0$ . A value of 0.860 reported in the literature was used as the density where there is no crystallinity.<sup>8</sup> Although in an ethylene homopolymer, 100% of the ethylene sequences have the capability to crystallize, it can be estimated from a density of 0.96 that less than 70% of the ethylene sequences did crystallize under the experimental conditions of this study. The percent crystallinity is expected to relate in some manner to the fraction of crystallizable ethylene as shown

$$\frac{d_{\text{obsd}} - d_0}{d_{100} - d_0} = f \left[ \frac{\sum_{n_2=n'+1}^{n_2=m} n_2 [X(E)_{n_2} X]}{[E]} \right] = f \left[ 1 - \frac{\sum_{n_1=1}^{n_1=n'} n_1 [X(E)_{n_1} X]}{[E]} \right] \quad (8)$$

where, as stated previously,  $n_2$  varies from  $n' + 1$  to " $m$ " and  $n_1$  varies from 1 to  $n'$ . It is likely that the relationship defined above is nonlinear because only a fraction of the sequences capable of crystallization will actually crystallize under the experimental conditions utilized and the overall percent of crystallization will also change with changing monomer content. The next requirement for establishing the relationship in eq 8 is to calculate sequence concentrations between  $n_1 = 1$  and selected values of  $n'$ . The fraction of ethylene in crystallizable sequences could then be determined as a function of  $n'$ . One approach to obtaining these necessary sequence concentrations for use in eq 8 is to find the best statistical fits for these copolymers by calculating the concentrations based on appropriate statistical models. The Bernoullian model has been previously used for such a purpose.<sup>10,11</sup> The fraction of  $X(E)_{n_1} X$  sequences from 1 to  $n'$  can be calculated and the relationship defined in eq 8 can be examined by plotting the fraction of crystallizable ethylene versus  $d_{\text{obsd}} - d_0 / d_{100} - d_0$  after assuming various values for  $n'$ . Once a best value of  $n'$  is established, eq 5 can be used to calculate the average number of sequences capable of crystallization per 100 copolymer repeat units (or per chain if end group concentrations are known). Some justification is required, however, before using the Bernoullian model for copolymers such as these, which were prepared with a variety of catalyst systems, many of which are multisited and therefore suspected to exhibit a broad range of reactivity ratio differences.

Table I contains triad distribution data determined from <sup>13</sup>C NMR for the various individual copolymers along with the best calculated Bernoullian and first-order Markovian statistical fits. The Bernoullian model assumes that the comonomer additions occur in a completely random fashion while the first-order Markovian model assumes that each chain addition depends upon the outcome of the previous monomer addition. There are conditions where the two models approach each other to the point of becoming equivalent as discussed in the Appendix. A priori, the first-order Markovian model is expected to be the more appropriate model for Ziegler-Natta catalyses because polymerization is controlled by the catalyst site. The Bernoullian model should be applicable only in those cases where the reactivity ratio product,  $r_1 r_2$ , is unity. In most of the copolymers examined in this study, Bernoullian statistics reproduced the profiles of the observed triad distributions well, while for some copolymers, first-order Markovian statistics gave an improved fit. In either case, the fits were close with the first-order Markovian fits representing only mild deviations from the Bernoullian case. The statistical analyses are given for comparison with the experimental data in Table I. It should be pointed out that the NMR triad data are an average result taken over somewhat heterogeneous molecular systems. In spite of this observation, Bernoullian and closely related first order Markovian statistics reproduce these average distributions well as shown in Table I. This success is likely related to the fact that the concentrations of the 1-olefin comonomer in these copolymers are at a level where the relative populations of the comonomers during polymerization have a greater influence upon the transition probabilities than do the intrinsic reactivity ratios. The net result is that the 1-olefin repeat units occur as EXE to an extent of 90% and more when the "X" concentrations are below 10 mol %. Bernoullian statistics become increasingly better approximations of the triad distributions as the 1-olefin comonomer concentrations get closer to zero. Between 0 and 5 mol %, the 1-olefin comonomer distributions can be approximated almost precisely by Bernoullian statistics even though the reactivity ratio product,  $r_1 r_2$ , may not be unity. This observation can be readily demonstrated by the equations for first-order Markovian transition probabilities<sup>12</sup> given in the Appendix.

Before proceeding further, it should be reported that some of the copolymer samples contained as much as 10% amorphous copolymer as produced during polymerization. This result was noted by first dissolving the copolymer samples in Decalin at approximately 130 °C and then allowing the samples to cool slowly to room temperature. The fraction that crystallized could then be separated from the amorphous copolymer, which remained in solution. Both fractions were then characterized by carbon-13 NMR. Bernoullian statistics reproduced the distributions of the isolated component copolymers as well as the composite. It is likely that these components are created at catalyst sites having different reactivity ratios;<sup>13</sup> nevertheless, the overall comonomer concentrations are such that the population differences are the overriding factors and Bernoullian statistics still satisfactorily reproduce the profile of the observed sequence distributions.

The simplest relationship that could be observed between density and sequence distributions would be density versus average ethylene sequence lengths. The triad distributions in Table I can be used to calculate observed average ethylene sequence lengths, which are listed in Table II. A graph showing density versus average ethylene sequence length is reproduced in Figure 1. Data are also

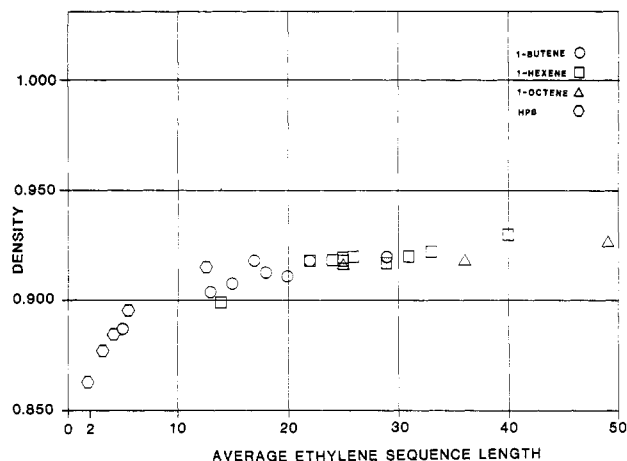


Figure 1. Average sequence length as a function of density for a series of ethylene-1-olefin copolymers.

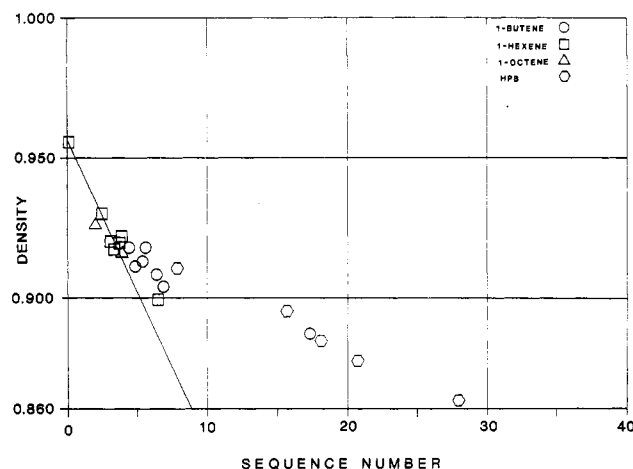


Figure 2. Sequence number as a function of density for a series of ethylene-1-olefin copolymers.

included for a series of hydrogenated polybutadienes furnished by Graessley,<sup>8,9</sup> where the average sequence lengths were determined from the triad distributions. The average sequence lengths for a 50/50 statistically random copolymer is 2.0. The observed data approach this value at a density of 0.86, which is the reported density for an amorphous copolymer.<sup>8</sup> This result lends credence to the conclusion that the observed sequence distributions for the series of ethylene-1-olefin copolymers examined in the study are not markedly different from statistically random distributions.

A second approach for testing the relationship between the observed sequence distributions and density would be an examination of density versus the sequence number. This graph is given in Figure 2 with the data of Graessley<sup>8,9</sup> also included. The points of this plot are converging toward a sequence number of 25, which is that for a 50/50 copolymer having a statistically random distribution. It is of interest to examine the region where low values of the sequence number occur. Initially, all of the *EXE* sequences will punctuate the long ethylene chain in such a way that shorter, yet still crystallizable, ethylene sequence lengths are produced. The onset of critically short ethylene sequence lengths between *EXE* punctuating sequences likely causes the curvature observed in the plot shown in Figure 2. In other words, the capability of comonomer incorporation to depress the density decreases as the 1-olefin content increases because the chain punctuating sequences begin to involve more than a single 1-olefin repeat unit. Later, the punctuating sequences involve

*EX(E)<sub>n</sub>XE* where *n* is less than *n'*. If one were to perform a linear extrapolation of the initial relationship between density and the sequence number down to a density of 0.86 for an amorphous copolymer, one would expect to obtain the sequence number for a totally amorphous copolymer that has only isolated and perfectly spaced comonomer insertions. The extrapolation is shown in Figure 2, and the resulting sequence number is 9. The average sequence length calculated from this value is 10, which should represent a reasonable estimate of *n'*. This result indicates that a 9 mol % ethylene-1-olefin copolymer would be completely amorphous if the 1-olefin repeat units were individually and uniformly spaced every 10 ethylene units.

Finally, the fraction of "crystallizable ethylene" is obtained by utilizing the statistical approach to calculate the percent ethylene in sequences of lengths from 1 to *n'*, as discussed previously. It is then possible to examine the relationships that develop between the percent crystallizable ethylene and the percent crystallinity defined in eq 8 as a function of *n'*. Even though the copolymer systems are not totally uniform compositionally, an average structure is compared to the density, which is also an average property of the system. Earlier investigators have also reported values for the minimum crystallizable sequence length in polyethylene. Their results are given below:

investigator	<i>n'</i> + 1
Natta et al. <sup>14</sup>	15
Burfield <sup>11</sup>	14
Killian <sup>15</sup>	13
Jackson <sup>10</sup>	8

As a consequence of these results and the relationship shown in Figure 2, values of *n'* of 6, 10, 12, and 18 were selected to test the behavior between the fraction of crystallizable ethylene and the observed crystallinity defined in eq 7. The fraction of ethylene in crystallizable sequences was calculated from

fraction of ethylene in crystallizable sequences =

$$1 - \sum_{n_1=1}^{n_1=n'} n_1 [X(E)_{n_1}X] / E \quad (9)$$

by obtaining the sum over *X(E)<sub>n<sub>1</sub></sub>X* from *n<sub>1</sub>* = 1 to *n'* values of 6, 10, 12, and 18 utilizing Bernoullian statistics for the sequence concentrations. These graphs are given in Figure 3, and it is clear that the relationship between the percent crystallinity and the fraction of "crystallizable ethylene" is nonlinear. Once again, data from a study of hydrogenated polybutadienes reported by Graessley<sup>8,9</sup> are included. One criteria for evaluating the observed plots is that the percent crystallinity is expected to be less than or equal to the fraction of "crystallizable ethylene" defined by eq 9, because the fraction of ethylene in sequences capable of crystallization cannot be less than the percent crystallinity if the branches cannot be accommodated in the crystalline structure. This limiting value for the percent crystallinity is shown by the linear heavy lines in Figure 3. Experimental conditions were chosen in this study where less than 70% of the crystallizable ethylene sequences would actually crystallize. For the relationships defined by *n'* = 18 and 12, the percent crystallinity becomes greater than the fraction of crystallizable ethylene at values of crystallizable ethylene below 20–25%. In the case of *n'* = 10, the fraction of crystallizable ethylene is more or less the same as the percent crystallinity at values below 15%. Clearly, *n'*s of 12 and 18 appear to be unreasonable possibilities. For *n'* = 10 to be a reasonable value, 100% of the available crystallizable ethylene se-

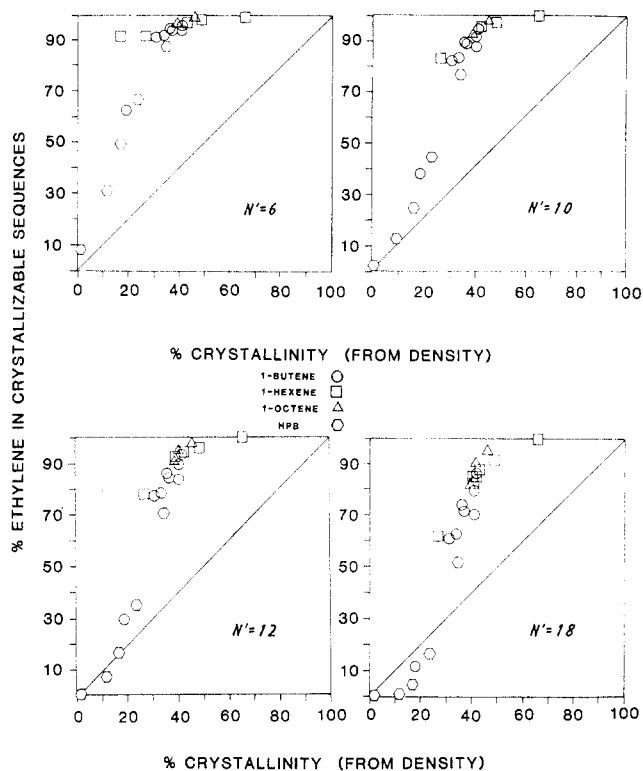


**Figure 3.** Percent crystallinity as a function of the percent ethylene in crystallizable sequences for  $n'$  values of 6, 10, 12, and 18.

quences must crystallize at a percent crystallinity below 15%. The relationship defined by  $n' = 6$  behaves properly. The fraction of crystallizable ethylene remains greater than the percent crystallinity throughout the range of crystallizable ethylene. In fact, the percent crystallinity starts at approximately 65% with a 99% crystallizable ethylene and decreases more rapidly than the fraction of crystallizable ethylene. At the lower densities, the percent crystallinity corresponds to only one-third or less of the fraction of crystallizable ethylene. This is the pattern of behavior that is expected. As the chain punctuation increases, fewer of the sequences capable of crystallization actually crystallize. A precise determination of  $n'$  would depend upon the accuracy of the NMR triad data for the hydrogenated polybutadienes. Because of the spread in sequence numbers for 1,4- versus 1,2-butadiene additions, this treatment cannot be used to pin down  $n'$  precisely. These crystallinity levels based on density do suggest that  $n'$  is lower than that previously reported and in a range between 6 and 10. The results for  $n'$  also strongly depend upon the method selected for determining the polyethylene crystallinities. Other methods that give lower values for the observed crystallinities, such as differential scanning calorimetry or infrared, would give correspondingly higher values for  $n'$ .

The sequence number for each of the ethylene-1-olefin copolymers can be used to determine the number of crystallizable sequences per 100 chain units provided reasonable values are available for  $n'$ . Either the X-centered or the E-centered triad distributions can be utilized separately to generate sequence numbers. Since the X-centered triads are also used to determine the mole fraction of "X", these same triads were utilized to determine the "X" sequence number. (The average difference between the sequence numbers as determined from the E-centered and X-centered runs is only 2.4%.) In principle, one would like to subtract from the sequence number all of the X-(E) $_n$ X sequences from  $n = 1$  to  $n = n'$ . This was done by

**Table III**  
Calculated Number of Crystallizable Ethylene Sequences/100 Chain Units versus Selected Values of " $n$ "<sup>a</sup>

sample	sequence number - $\sum X(E)_n X$			
	XEX $n' = 1$	$n = 1^b$ $n' = 6$	$n = 1^b$ $n' = 8$	$n = 1^b$ $n' = 10$
I	0.1	0.1	0.1	0.1
J	2.2	1.9	1.8	1.7
W	2.0	1.8	1.7	1.7
K	2.7	2.3	2.1	2.0
L	3.3	2.7	2.5	2.3
M	2.9	2.4	2.3	2.1
A	3.2	2.7	2.5	2.4
N	3.4	2.7	2.5	2.2
O	3.2	2.6	2.4	2.2
P	3.4	2.7	2.4	2.2
B	4.8	3.5	3.1	2.7
C	3.8	3.0	2.7	2.5
Q	3.6	2.8	2.5	2.3
R	3.6	2.9	2.6	2.4
S	3.7	3.0	2.7	2.5
X	2.5	2.2	2.1	1.9
T	3.3	2.7	2.5	2.4
U	3.8	3.1	2.9	2.6
D	5.0	3.8	3.4	3.0
E	4.8	3.7	3.3	3.0
F	6.0	4.2	3.7	3.2
G	6.1	4.3	3.7	3.2
V	6.0	4.2	3.6	3.1
HPB-1.262°	4.2	3.3	3.0	2.8
H	13.2	5.4	4.0	3.0
HPB-1.015	8.6	5.6	4.9	4.3
HPB-1.387°	10.3	4.9	3.8	3.0
HPB-1.086	12.3	4.0	2.7	1.8
HPB-1.291	18.4	3.9	2.7	2.2

<sup>a</sup> Data arranged in order of decreasing density. <sup>b</sup> Experimental values of XEX were used with the sequences from  $n = 2$  to  $n'$  calculated statistically. <sup>c</sup> Experimental values of XEX were not used.

rearranging eq 5 to define the "number of crystallizable sequences per 100 chain units"

$$\text{number crystallizable sequences per 100 units} = \frac{\text{sequence number} - 100[XEX + XEEX + \dots + X(E)_{n'}X]}{100} \quad (10)$$

where, once again,  $n'$  is the maximum E sequence length that will not crystallize. Notice that eq 10 goes to zero whenever the longest uninterrupted ethylene sequence is  $n'$ . As the 1-olefin concentrations increase, the "number of crystallizable sequences/100 units" should first increase, reach a maximum, and then finally approach zero as the copolymer chain becomes totally amorphous.

The relationship between density and chain punctuation as defined above was investigated by plotting the observed densities versus "the number of crystallizable ethylene sequences per 100 units" at  $n' = 6$  and 10 as shown in Figure 4. The data for values of  $n'$  of 6, 8, and 10 are given in Table III. The data for the series of hydrogenated polybutadienes from Graessley<sup>8,9</sup> were also included. As expected, the number of crystallizable sequences per 100 chain units increase as the minimum crystallizable sequence length decreases. It is interesting to note that a density can be identified where the maximum number of crystallizable sequences occurs. For  $n' = 10$ , the maximum number of crystallizable sequences is found at a density of approximately 0.905. It is only slightly below 0.900 for  $n' = 8$ . At densities below these values, the copolymer chains have increasing numbers of ethylene runs incapable of crystallization located between ethylene runs of sufficient length to crystallize.

### Summary and Conclusions

The value of the "run number" and "sequence number"



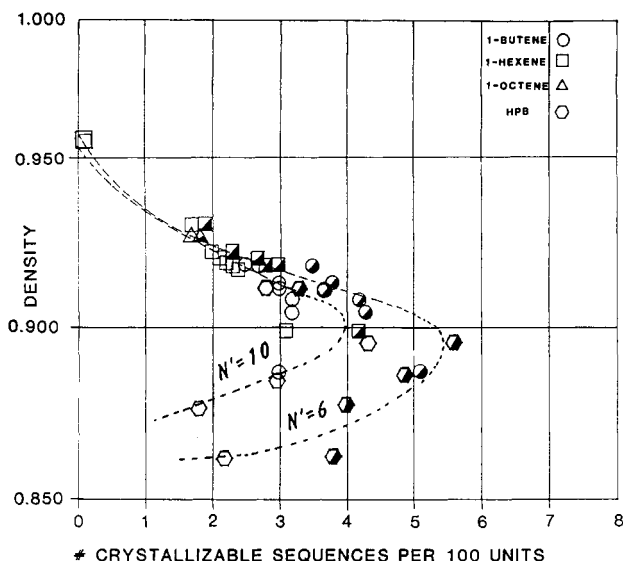


Figure 4. Number of crystallizable sequences per 100 chain units as a function of density for a series of ethylene-1-olefin copolymers.

concepts in copolymer characterization has hopefully been demonstrated. Some account of contiguous and closely spaced chain disrupting repeat units must be made when copolymer compositions are related to properties such as crystallinity. In this study of linear low density polyethylenes, it is shown that a nonlinear relationship exists between the percent crystallinity and the fraction of ethylene in sequences capable of crystallization. The maximum ethylene sequence length between 1-olefin repeat units that fails to crystallize under any conditions appears to be between 6 and 10 in agreement with Jackson<sup>10</sup> and a somewhat lower value than reported recently.<sup>11</sup> More importantly, the maximum number of "crystallizable ethylene" sequences per chain occurs around a density of 0.90. Finally, it has been reaffirmed that the crystallinity of linear low density polyethylenes is related to the arrangements and frequencies of chain disrupting 1-olefin derived repeat units and is not necessarily a strict function of branch length for ethyl, butyl, and hexyl branches.

**Acknowledgment.** We wish to express our appreciation to Dr. W. W. Graessley for reading the manuscript and offering a number of helpful discussions. We are particularly indebted to Professor L. Mandelkern for stimulating and fruitful discussions. Professor R. S. Stein and Dr. F. C. Stehling also contributed through encouraging comments and helpful discussions. Appreciation is also expressed to Miguel Meusz for his careful work in obtaining the carbon-13 NMR spectra.

## Appendix

Equations for the first-order Markovian transition probabilities<sup>12</sup> have been rearranged as follows to illustrate the effects of contributions from kinetic versus comonomer population differences upon the various transition probabilities

$$P_{11} = \frac{r_1}{[r_1 + (x_2/x_1)_{\text{feed}}]} \quad (11)$$

$$P_{12} = \frac{1}{[1 + r_1(x_1/x_2)_{\text{feed}}]} \quad (12)$$

$$P_{21} = \frac{1}{[1 + r_2(x_2/x_1)_{\text{feed}}]} \quad (13)$$

$$P_{22} = \frac{r_2}{[r_2 + (x_1/x_2)_{\text{feed}}]} \quad (14)$$

where "1" represents ethylene and "2" represents the 1-olefin and  $r_1 = k_{11}/k_{12}$  and  $r_2 = k_{22}/k_{21}$ . It can be seen in Equations 9 and 11 that both  $P_{11}$  and  $P_{21}$  approach 1 as " $x_2$ " approaches zero. In a similar manner, both  $P_{22}$  and  $P_{12}$  approach zero as " $x_2$ " approaches zero. Thus copolymer systems can be approximated by Bernoullian statistics as  $x_2$  approaches zero because, as sets, both  $P_{11}$ ,  $P_{21}$  and  $P_{22}$ ,  $P_{12}$  are approaching similar values. The applicability of Bernoullian statistics to these systems can therefore be demonstrated by the  $P_{11}/P_{21}$  and  $P_{22}/P_{12}$  ratios, which are expressed in diad and monomer concentrations.<sup>16</sup> A first-order Markov process reduces to Bernoullian when

$$P_{11}/P_{21} = \frac{2[X][EE]}{[E][EX + XE]} = 1 \quad (15)$$

$$P_{22}/P_{12} = \frac{2[E][XX]}{[X][EX + XE]} = 1 \quad (16)$$

The  $P_{11}/P_{21}$  ratio is close to unity for the  $n$ -ad distributions in Table I because both transition probabilities are above 0.9 where possible real differences are not manifested in the observed transition probability ratio as shown by the similarities in the observed Bernoullian versus first-order Markovian fits. The  $P_{22}/P_{12}$  ratio is not close to unity because both transition probabilities are close to zero where differences are accentuated by the respective ratio because of either real differences or scatter in the experimental data. The similarities in the Bernoullian and Markovian fits result from the fact that  $P_{11}$  and  $P_{21}$  are above 0.9 while  $P_{22}$  and  $P_{12}$  are, correspondingly, below 0.1. For example, it can be seen for polymer "F" that Bernoullian statistics closely approximate the observed triad distribution. When testing for the suitability of Bernoullian statistics through a first-order Markov trial utilizing eq 13 and 14, one finds that eq 13 gives a ratio of 0.99 while eq 14 gives 0.54. The first-order Markovian transition probabilities for eq 14 are  $P_{22} = 0.04$  and  $P_{12} = 0.07$ . In spite of this difference, a reasonable Bernoullian fit was obtained because  $P_{22}$  and  $P_{12}$  were close to zero. As shown in Table I by the Bernoullian versus observed triad distributions, reactivity ratio differences are not manifested within three significant figures for the observed sequence distributions when the 1-olefin comonomer is in a concentration range below 5 mol %. The differences between the observed and Bernoullian distributions become particularly small when the reactivity ratios do not markedly deviate from random kinetics in the first place. The importance of this result is that either Bernoullian or closely related first-order Markovian statistics can be used to predict sequence concentrations in linear low density polyethylenes for those sequences which cannot be measured directly by NMR. Therefore, the fraction of ethylene in crystallizable sequences can be calculated for various values of  $n_1$  and possible relationships tested in eq 7 for the best value of  $n'$ .

**Registry No.** (Ethylene)(1-butene) (copolymer), 9019-29-8; (ethylene)(1-hexene) (copolymer), 25213-02-9; (ethylene)(1-octene) (copolymer), 26221-73-8.

## References and Notes

- Harwood, H. J.; Ritchey, W. M. *Polymer Lett.* **1964**, *2*, 601.
- Randall, J. C.; Hsieh, E. T. *NMR and Macromolecules*, ACS Symposium Series 247, American Chemical Society: Washington, D.C., 1984; Chapter 9.
- Frisch, H. L.; Mallows, C. L.; Bovey, F. A. *J. Chem. Phys.* **1966**, *45*, 1565.
- Randall, J. C. *Polymer Sequence Determination: Carbon 13 NMR Method*; Academic: New York, 1977; p 33.
- Ray, G. J.; Spanswick, J.; Knox, J. R.; Serres, C. *Macromolecules* **1981**, *14*, 1323.
- Hsieh, E. T.; Randall, J. C. *Macromolecules* **1982**, *15*, 353.
- Hsieh, E. T.; Randall, J. C. *Macromolecules* **1982**, *15*, 1402.



- (8) Krigas, T. M.; Carella, J. M.; Struglinski, M. J.; Crist, B.; Graessley, W. W. *J. Polym. Sci., Poly. Phys. Ed.* **1985**, *23*, 509.
- (9) Graessley, W. W., private communication.
- (10) Jackson, J. F. *J. Polym. Sci., Part A* **1963**, *1*, 2119.
- (11) Burfield, D. R. *Makromol. Chem.* **1985**, *186*, 2657.
- (12) Ham, G. E. *Copolymerization*; Interscience: New York, 1964; Vol. XVIII, Chapter I.
- (13) Usami, T.; Gotoh, Y.; Takayama, S. *Macromolecules* **1986**, *19*, 2722.
- (14) Natta, G.; Mazzanti, G.; Valvassori, A.; Sartori, G.; Morero, D. *Chim. Ind. (Milan)* **1960**, *42*, 125.
- (15) Killian, H. G. *Kolloid-Z.* **1963**, *189*, 23.
- (16) Kakugo, M.; Naito, Y.; Mizunuma, K.; Miyatake, T. *Macromolecules* **1982**, *15*, 1150.

## Characterization of a Polymer Blend by the Spin Label Method: Concentration of Poly(methyl methacrylate) in a Blend with Poly(vinylidene fluoride)

Shigetaka Shimada,\* Yasurō Hori, and Hisatsugu Kashiwabara

*Nagoya Institute of Technology, Gokiso-cho, Nagoya 466, Japan.*

*Received September 30, 1987; Revised Manuscript Received May 18, 1988*

**ABSTRACT:** The electron spin resonance line shape of nitroxide radical labels attached to poly(methyl methacrylate) (PMMA) side chains in blends with poly(vinylidene fluoride) (PVDF) was studied as a function of PVDF content. The principal values are anisotropic hyperfine splitting ( $A_z$ ) due to the nitrogen nucleus and the line width increase with PVDF content. The increase,  $\Delta A_z$ , can be attributed to the effect of the electric field of a PVDF chain in a molecularly compatible system. The outermost splitting width ( $2A_z$ ) observed at  $-196^\circ\text{C}$  was a good measure of PMMA concentration in the molecularly mixed phase. Estimation of the concentrations of both phases in a phase-separated system as a function of annealing temperature indicated that an upper critical solution temperature (UCST) exists at about  $100^\circ\text{C}$ .

### Introduction

Many authors have studied blends of poly(methyl methacrylate) (PMMA) and poly(vinylidene fluoride) (PVDF).<sup>1</sup> The general conclusion is that these components are compatible in an amorphous state, i.e., above the melting point of PVDF ( $T_m \approx 170^\circ\text{C}$ ). Below  $T_m$ , the PVDF chain crystallizes from a molten blend, especially at high PVDF content. Bernstein et al.<sup>1b</sup> and Hirata and Kotaka<sup>1c</sup> observed lower critical solution temperature behavior at temperatures above  $200^\circ\text{C}$ . On the other hand, Saito et al.<sup>1i</sup> concluded that phase separation takes place at an upper critical solution temperature (UCST) around  $100^\circ\text{C}$ , based on the crystallization of PVDF from the melt at various temperatures. Hahn et al.<sup>1j</sup> also concluded that the amorphous PVDF interphase separates from crystalline and mixed amorphous regions. Blends of PMMA and PVDF are generally composed of a crystalline phase of PVDF and a liquidlike amorphous phase; the amorphous phase may be composed of PMMA-rich and PVDF-rich phases in a phase-separated system.

Since it is not certain that the amorphous region is completely phase-separated, it is important to estimate unambiguously the concentration of the respective chains in both phases. The ESR method is a simple and effective way of determining the molecular structure and molecular motion of only one kind of a spin-labeled polymer chain in a complicated system.<sup>2</sup>

Our aim in this study was to determine the concentration of spin-labeled PMMA in a PMMA/PVDF blend and to assess the translational diffusion of PMMA chains in relation to the molecular compatibility of the components.

### Experimental Section

**Materials.** PVDF was Kynar 731 powder (Pennwalt Chemical Co., Ltd.). Spin-labeled PMMA was prepared by anionic copolymerization of MMA monomer (Tokyo Kasei Co., Ltd.) with a labeled monomer, 4-(methacryloyloxy)-2,2,6,6-tetramethyl-

piperidine,<sup>3</sup> using butyllithium catalyst at  $-78^\circ\text{C}$ . The mole ratio of labeled monomer to MMA monomer was less than 1:250. The weight-average molecular weight,  $M_w$ , and the number-average molecular weight,  $M_n$ , are, respectively, 462 000 and 80 800 for PVDF and 125 000 and 29 000 for PMMA. The tacticity of the PMMA, determined by high-resolution  $^1\text{H}$  NMR,<sup>4</sup> was isotactic 88%, heterotactic 4%, and syndiotactic 8% in terms of triads. Another probe, 4-hydroxy-2,2,6,6-tetramethylpiperidine-1-oxyl (TANOL) was also used to confirm the intermolecular interaction between nitroxide radicals and polymer chains.

**Preparation of Blends.** Blends were made by mixing spin-labeled PMMA and PVDF in the ratios 70:30, 50:50, 33:67, and 11:89 by weight. Films of blends and of spin-labeled PMMA were prepared by casting from  $\sim 3$  wt % acetone solution at  $50^\circ\text{C}$ . The films were dried under vacuum for more than 1 day at room temperature. Films of spin-probed PMMA and spin-probed PVDF ( $\sim 6 \times 10^{-4}$  mol of Tanol per mole of polymer) were prepared by the same method.

**ESR Measurements.** Samples were stacked in ESR sample tubes evacuated to  $10^{-5}$  mmHg. ESR measurements were carried out with a JEOL FE3XG spectrometer with a connected MEL-COM 70/25 computer. The signal of diphenylpicrylhydrazyl (DPPH) was used as a  $g$ -value standard. The magnetic field sweep was calibrated with the known splitting constant of  $\text{Mn}^{2+}$ .

**Simulation.** Computer simulation was carried out in order to obtain the principal values of  $g$  and  $A$  tensors and the line width. Since it was reasonable to assume that the nitroxide radicals have a completely random orientation, the  $g$  and  $A$  values could be computed from eq 1 and 2,<sup>5</sup> choosing the 8100 sets of

$$g = (g_x^2 \sin^2 \theta \sin^2 \phi + g_y^2 \sin^2 \theta \cos^2 \phi + g_z^2 \cos^2 \theta) \quad (1)$$

$$A = (g_x^2 A_x^2 \sin^2 \theta \sin^2 \phi + g_y^2 A_y^2 \sin^2 \theta \cos^2 \phi + g_z^2 A_z^2 \cos^2 \theta)^{1/2} \quad (2)$$

( $\theta, \phi$ ) in a solid angle of  $\pi/2$ , where  $g_x, g_y$ , and  $g_z$  are the principal values of the  $g$  tensor and  $A_x, A_y$ , and  $A_z$  are those of the  $A$  tensor due to the nitrogen nucleus. It was also assumed that the principal directions of the  $g$  and  $A$  tensors coincided. Several theoretical spectra were calculated by gradually changing the principal values and the line width of the Gaussian line shape function. These spectra were recorded on an X-Y plotter and